Congenital Heart Disease

Tech Science Press

DOI: 10.32604/chd.2023.023542

check for updates

ARTICLE

Assessment of Intracardiac and Extracardiac Deformities in Patients with Various Types of Pulmonary Atresia by Dual-Source Computed Tomography

Wenlei Qian[1,#], Xinzhu Zhou[2,#], Ke Shi[1], Li Jiang[1], Xi Liu[3], Liting Shen[1] and Zhigang Yang[1,*]

[1]Department of Radiology, West China Hospital, Sichuan University, Chengdu, China

[2]Department of Radiology, Chengdu Women's and Children's Central Hospital, School of Medicine, University of Electronic Science and Technology of China, Chengdu, China

[3]Department of Radiology, Peking University Cancer Hospital and Institute, Beijing, China

[*]Corresponding Author: Zhigang Yang. Email: yangzg666@163.com

[#]These authors contributed equally to this work and should be considered the co-first authors

Received: 25 May 2022 Accepted: 29 November 2022

ABSTRACT

Background: Pulmonary atresia (PA) is a group of heterogeneous complex congenital heart disease. Only one study modality might not get a correct diagnosis. This study aims to investigate the diagnostic power of dual-source computed tomography (DSCT) for all intracardiac and extracardiac deformities in patients with PA compared with transthoracic echocardiography (TTE). **Materials and Methods:** This retrospective study enrolled 79 patients and divided them into three groups according to their main diagnosis. All associated malformations and clinical information, including treatments, were recorded and compared among the three groups. The diagnostic power of DSCT and TTE on all associated malformations were compared. The surgical index (McGoon ratio, pulmonary arterials index (PAI), and total neopulmonary arterial index) and radiation dose were calculated on the basis of DSCT. **Results:** Of the patients, 32, 30, and 17 were divided into the groups of PA with ventricular septal defect (VSD), PA with VSD and major aortopulmonary collateral arteries, and PA with other major malformations, respectively. Consequently, 182, 162, and 13 intracardiac, extracardiac, and other major malformations were diagnosed, respectively. Moreover, DSCT showed a better diagnostic performance in extracardiac deformities (154 *vs.* 117, $p < 0.001$), whereas TTE could diagnose intracardiac deformities better (159 *vs.* 139, $p = 0.001$). The McGoon ratio, PAI, and treatment methods were significantly different among the three groups ($p = 0.014$, $p = 0.008$, and $p = 0.018$, respectively). **Conclusion:** More than one imaging modality should be used to make a correct diagnosis when clinically suspecting PA. DSCT is superior to TTE in diagnosing extracardiac deformities and could be used to roughly calculate surgical indices to optimize treatment strategy.

KEYWORDS

Pulmonary atresia; complex congenital heart diseases; dual-source computed tomography; transthoracic echocardiography

1 Introduction

Pulmonary atresia (PA) is identified as a group of heterogeneous congenital heart disease (CHD) whose most important feature is the lack of continuity between the pulmonary arteries and the right ventricle. Hence,

PA is nearly accompanied by other congenital intracardiac and extracardiac abnormalities [1–3]. PA is rare but fatal [4]. The survival rate is low without early interventions. Early and late mortality is high in all types of PA [5]. In fact, even when patients underwent operation, the success rate of surgery was low during the first 30 years after this disease was reported [6,7]. However, because of the histologic study of major aortopulmonary collateral arteries (MAPCAs) and native pulmonary arteries (NPA), and accumulated knowledge of the blood supply of the lungs [8,9], the survival rate is gradually increasing [10,11]. Thus, the condition of NPA, MAPCAs, and other deformities are of the highest importance for surgical strategy and management [6,12].

Transthoracic echocardiography (TTE) is a first-line CHD examination that could investigate intracardiac deformities well. However, TTE is not very useful for extracardiac deformities that are crucial for surgical choices. Cardiac computed tomography is an excellent imaging modality in patients with CHD, which could reliably visualize pulmonary arterial supply [13,14]. Additionally, dual-source computed tomography (DSCT) broadens its application range because of its lower radiation dose and higher density and spatial resolution [15]. To date, only a few studies focusing on PA with ventricular septal defect (VSD) and MAPCAs explored the value of DSCT for diagnosing PA [16,17]. However, PA is not just one type. Thus, this study divided PA patients into three groups according to their main diagnosis. The aims of this study were comparing the differences of the three groups and exploring the DSCT diagnostic power for all intracardiac and extracardiac deformities in different PA patients.

2 Materials and Methods

2.1 Study Population

This study retrospectively enrolled 79 PA patients with various malformations who underwent preoperative DSCT and TTE examinations from June 2012 to December 2020 at the medical center of this study. The inclusion criteria were (1) patients who underwent surgery or cardiac catheterization with angiography (CCA) with PA included as the final diagnoses and (2) those who underwent both DSCT and TTE examinations before surgery or CCA, with the time interval between the two tests not exceeding 1 month. The exclusion criteria were (1) incomplete medical records and (2) the image quality not meeting the diagnosis requirement. Depending on the main diagnosis, all patients were divided into three groups: (1) patients with PA and ventricular septal defect (PA/VSD), (2) patients with PA with VSD and major aortopulmonary collateral arteries (PA/VSD/MAPCAs), and (3) patients with PA with other major malformation (such as PA with single atrium, PA with single ventricle, PA with intact ventricular septum, and PA with double outlet left/right ventricle).

This study was in line with the principles of the Declaration of Helsinki and approved by the Institutional Ethics Committee of West China Hospital, Sichuan University (Chengdu, China; No. 14-163), with a waiver of informed consent due to the retrospective nature. All personal details of any patients have been removed carefully before submission.

2.2 Scanning Protocol

All DSCT scans were performed on the same type of machines (Somatom Definition; Siemens Medical Solutions, Forchheim, Germany). Patients aged >5 years were trained to hold their breath during the examination. When necessary, patients aged <5 years and who could not cooperate were given short-term sedation (chloral hydrate; 10% concentration; dose, 0.5 mL/kg). The scan direction was craniocaudal, and the scan range was from the inlet of the thorax to 2 cm below the diaphragm level. A nonionic contrast agent (iopamidol, 370 mg/mL; Bracco, Italy) was given intravenously (1.5 mL/kg body weight) at a rate of 1.2–2.5 mL/s, followed by 20 mL of saline solution. Automated bolus-tracking software was utilized to start the scan when the region of interest attenuation threshold reached 100 HU following a delay of 5 s. The region of interest was set in the descending aorta. The protocol parameters (flash chest pain

electrocardiogram; ECG) were as follows: tube voltage (70−120 kV; controlled by CARE KV), reference retube current (100–400 mAs, reduced by CARE Dose 4D), gantry rotation time (0.33 s), and pitch (0.2–0.5; adapted to heart rate). Moreover, the field of view was adjusted to body size.

Images were reconstructed with a slice thickness and an increment of 0.75 and 0.5 mm, respectively. The convolution kernel was I26f medium smooth ASA. Sinogram-affirmed iterative reconstruction (strength, 3) and a retrospective ECG-gated technique were used to improve image quality. All image data were transferred to a workstation (Syngo; Siemens Medical Systems, Forchheim, Germany). Several postprocessing methods (e.g., multiplanar reformations, volume rendering, and maximum intensity projection) were applied to complete image analysis [16].

Image analysis

All DSCT images were retrospectively reviewed by two veteran radiologists without knowing the surgery or CCA results. The main abnormalities were carefully reviewed at the workstation using different postprocessing methods. The diameters of the left pulmonary arterials, right pulmonary arterials, MAPCAs, and descending aorta were recorded similarly to that in reference [16]. The only difference in the measurement was that the main pulmonary artery (MPA) if existing was located at the maximum of MPA. All measurements avoided narrow places. The body surface area was calculated by the Stevenson formula. The McGoon ratio, pulmonary arterials index (PAI), and total neopulmonary arterial index (TNPAI) were calculated in the standard ways.

All detected malformations were recorded from long and short cardiac axis view at the xiphoid process, parasternum, and suprasternal fossa by an experienced echocardiography practitioner. The inferior vena cava long axis view, three vessels and trachea view were used to detect the development of pulmonary artery and collateral circulation.

2.3 Radiation Dose Estimation

DSCT examinations strictly adhered to the principle of “as low as reasonably achievable”. Tube voltage, tube current, and pitch were adjusted on the basis of every patient’s individual circumstance to lower the dose as much as possible as illustrated above. Meanwhile, the ECG-gated technique was used to reduce the radiation dose. Volume CT dose index and dose length product were recorded. Patients of different ages reacted differently to the radiation dose. Hence, the effective dose with different conversion coefficients was calculated as k ($effective\ dose = dose\ length\ product \times k$) on the basis of the 2007 recommendations of the International Commission on Radiological Protection [18,19].

2.4 Statistical Analysis

The Statistical Package for the Social Sciences software for Windows (version 25.0, SPSS Inc., Chicago, IL, USA) was used for statistical analysis. The Shapiro–Wilk test was used to test the normality of the variables. Bartlett’s test was used to assess the homogeneity of the variance. Categorical variables (such as sex, symptoms and treatments) were measured as percentages and compared by Fisher’s exact or chi-square test, depending on the expected frequencies. Continuous variables (such as age, BMI, heart rate, SpO_2, McGoon, PAI and so on) were recorded as means with standard deviations or medians with interquartile ranges (IQRs) and were compared by one-way analysis of variance (ANOVA) followed by least-significant difference (LSD) post hoc test (normally distributed continuous variables and the variance is homogeneous) or the Kruskal–Wallis test (non-normally distributed continuous variables). Independent Student’s t-test was used to compare TNPAI. The sensitivity, specificity, positive predictive value, and negative predictive value for DSCT and TTE were evaluated for the intracardiac and extracardiac deformities in each group. The interobserver reproducibility of McGoon ratio, PAI, and TNPAI was tested by intraclass correlation coefficient (ICC) by using 32 randomly chosen patients. The

ICC score of >0.75 was taken for satisfactory agreement. Furthermore, a two-tailed p value of <0.05 was considered statistically significant in all statistical analyses.

3 Results

3.1 Baseline Characteristics of all Patients with PA

This study consecutively included 79 (female, 47; 59.5%) patients. The patients' ages ranged from 19 days to 35 years old; the mean age was 26 (IQR, 10.0–58.0) months. The mean body mass index, heart rate and respiratory rate were 15.2 (IQR, 13.7–17.0) kg/m^2, 117 ± 18 bpm and 28 ± 5 bpm, respectively. The mean preoperative and postoperative SpO_2 was 79.3% ± 10.1% and 94.7% (IQR, 84.0%–97.0%) (if patients underwent operation), respectively. Furthermore, the mean postoperative SpO_2 was significantly higher than the mean preoperative SpO_2 ($p < 0.001$).

3.2 Basic Characteristics among Three Subgroups

Of the patients, 32, 30, and 17 were divided into the groups of PA/VSD/MAPCAs (Figs. 1 and 2), PA/VSD (Fig. 3), and the PA group with other major malformations (i.e., seven patients with a double outlet of the right ventricle, three patients with single ventricle, two patients with single ventricle and single atrium, one patient with single ventricle and mitral valve atresia, and four patients with intact ventricle (Fig. 4)), respectively. For basic clinical characteristics, most indices showed no significant difference except for age and respiratory rate. Most patients had one or more symptoms, while a few patients showed no associated symptoms. Symptoms among the three groups were not significantly different; the most frequent symptom was cyanosis (Table 1).

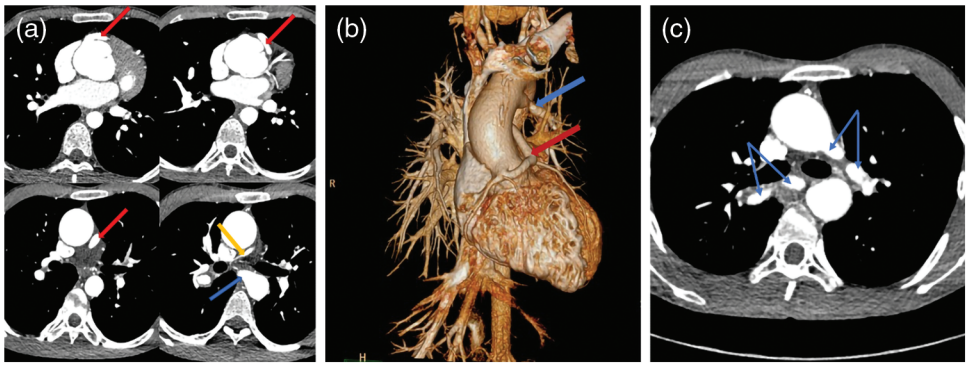

Figure 1: A pulmonary atresia (PA) patient with ventricular septal defect (VSD) and major aortopulmonary collateral arteries (MAPCAs). A source of the blood supply of his right lung came from the right coronary artery (CA, red arrows). His right pulmonary artery (yellow arrow) and left pulmonary artery (not shown) developed poor, leading to MAPCAs growing (blue arrows). (a) The transverse image of the right coronary artery and one of MAPCAs. (b) The volume rendering (VR) of the CA and a MAPCA. (c) The MAPCAs supply blood to the lungs

3.3 The Treatment Choices and Surgical Indices among Three Subgroups

The choices of the three groups were significantly different ($p = 0.018$). All PA/VSD patients underwent surgery. PA/VSD group and PA patients with other major malformations group underwent more staged surgeries and PA/VSD/MAPCAs group underwent slightly more one-staged surgeries (Fig. 5). For quantitative parameters that are of guiding significance for surgical options, The PAI of PA/VSD/MAPCAs group was significantly different from the other two groups, while the PAI of PA/VSD and PA patients with other major malformations showed no significant difference (132.77 ± 102.01 *vs.* 213.49 ±

110.66 *vs.* 218.82 ± 106.41, $p = 0.008$). McGoon was significantly different between PA/VSD patients and PA/VSD/MAPCAs patients (1.74 ± 0.48 *vs.* 1.35 ± 0.59, $p = 0.014$). However, McGoon and TNPAI showed no significant difference between PA/VSD/MAPCAs and PA patients with other major malformations (Table 1). All ICC scores of the two radiologists were >0.75, showing great repeatability (Table 2).

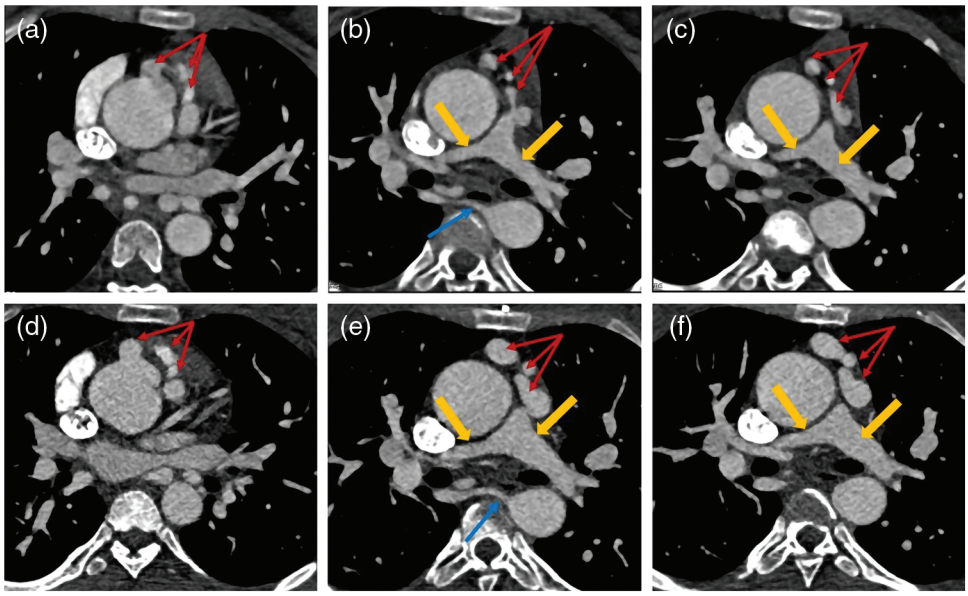

Figure 2: Two sets of images of a PA/VSD/MAPCAs patient. Images of (a–c) were captured in 2013 and (d–f) were taken in 2019. Unlike with the patient in Fig. 1, the blood supply of this patient lungs depended more on right coronary artery (CA, red arrows) than MAPCA (blue arrows). After six years, the right CA dilated more distinctly, while the left/right pulmonary artery (LPA/RPA, yellow arrows) and MAPCA changed little. (a–c): CA = 0.53 cm, MAPCA = 0.41 cm, LPA = 0.51 cm, RPA = 1.25 cm; (d–f): CA = 1.20 cm, MAPCA = 0.52 cm, LPA = 0.66 cm, RPA = 1.53 cm

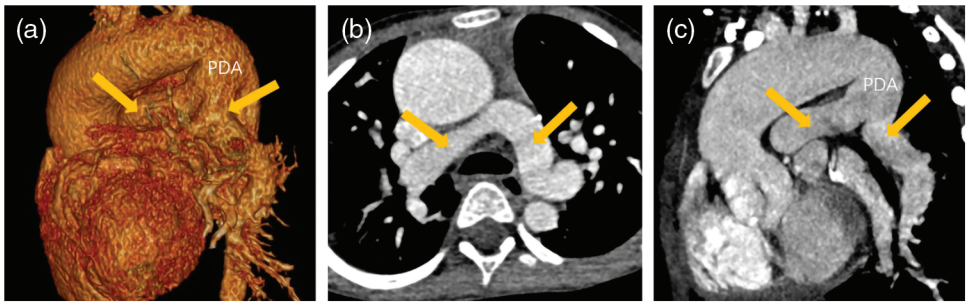

Figure 3: A patient with PA/VSD. The blood supply of his lungs came from patent ductus arteriosus (PDA). His ascending aorta and aortic arch dilated obviously. His PDA was tube-shaped and his left/right pulmonary artery (yellow arrows) developed well. (a) The VR image of PDA and left/right pulmonary. (b) The transverse image of left/right pulmonary. (c) The reconstruction image of PDA and left/right pulmonary

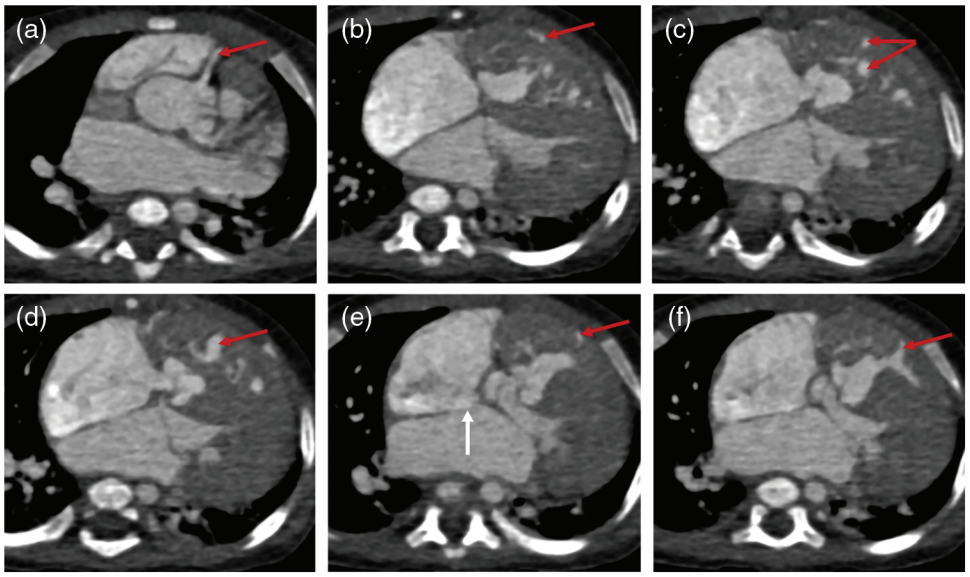

Figure 4: The images of a PA patient with intact ventricular septum (IVS) complicated by right ventricular dependent coronary circulation (RVDCC). PA/IVS/RVDCC is a rare and fatal type of PA whose treatments differ from other types of PA. The tricuspid valve and right ventricle of this patient developed poorly. Besides, he had atrial septal defect (white arrow). The red arrows show that the right coronary artery (red arrow) communicates with the right ventricle

Table 1: Baseline characteristics of three groups

Characteristics	PA/VSD (n = 32)	PA/VSD/MAPCAs (n = 30)	PA with other major malformation (n = 17)	*p* values
Age, months	10.9 (6.8–44.0)*	51.0 (23.8–107.0)*§	19.0 (12.0–43.0)§	0.000
Male, n (%)	10 (31.3)	13 (43.3)	9 (52.9)	0.310
BMI (kg/m^2)	15.7 (14.1–17.0)	14.7 (13.3–18.4)	14.5 (13.7–17.0)	0.584
Heart rate (bpm)	121 ± 19	112 ± 19	116 ± 12	0.130
Respiratory rate (bpm)	29 ± 6*	25 ± 3*§	29 ± 4§	0.003
Preoperative SpO_2 (%)	77.3 ± 11.0	81.9 ± 9.5	78.3 ± 8.6	0.186
Postoperative SpO_2 (%)	94.8 (87.0–96.2)	96.0 (82.0–97.2)	86.1 (82.0–95.0)	0.172
Heart murmurs, n (%)	28 (87.5)	28 (93.3)	15 (88.2)	0.711
Symptoms, n (%)				
Cyanosis	28 (87.5)	24 (80.0)	16 (94.1)	0.451
Post-exercising tachypnea	10 (31.3)	13 (43.3)	4 (23.5)	0.365
prone to colds	9 (28.1)	6 (20.0)	4 (23.5)	0.794
Growth retardation	7 (21.9)	7 (23.3)	5 (29.4)	0.889
Squatting	6 (18.8)	4 (13.3)	0	0.168
Acropachy	2 (6.3)	4 (13.3)	0	0.255
Dyspnea	3 (9.4)	5 (16.7)	1 (5.9)	0.598

(Continued)

Table 1 (continued)

Characteristics	PA/VSD (n = 32)	PA/VSD/MAPCAs (n = 30)	PA with other major malformation (n = 17)	*p* values
No symptom	4 (13.8)	3 (10.0)	1 (5.9)	0.895
Treatments, n (%)				0.018
Staged surgery	19 (59.4)	10 (34.5)	11 (60.0)	
One-staged surgery	13 (40.6)	14 (44.8)	4 (26.7)	
CCA only	0	6 (20.7)	2 (13.3)	
McGoon	1.74 ± 0.48*	1.35 ± 0.59*	1.62 ± 0.45	0.014
PAI	213.49 ± 110.66*	132.77 ± 102.01*§	218.82 ± 106.41§	0.008
TNPAI	-	223.71 ± 125.94	193.10 ± 65.62	0.572

Note: Values are means standard deviations, media (Q1–Q3) or n (%). *p* value was the result of ANOVA analysis, Kruskal-Wallis test or Student's *t*-test/Chi-square/Fisher's exact test between subgroups. * means $p < 0.05$ between PA/VSD and PA/VSD/MAPCAs; § means $p < 0.05$ between PA with other major deformities and PA/VSD/MAPCAs. Abbreviations: CCA, cardiac catheterization with angiography; PAI, pulmonary arterials index; TNPAI, total neopulmonary arterial index.

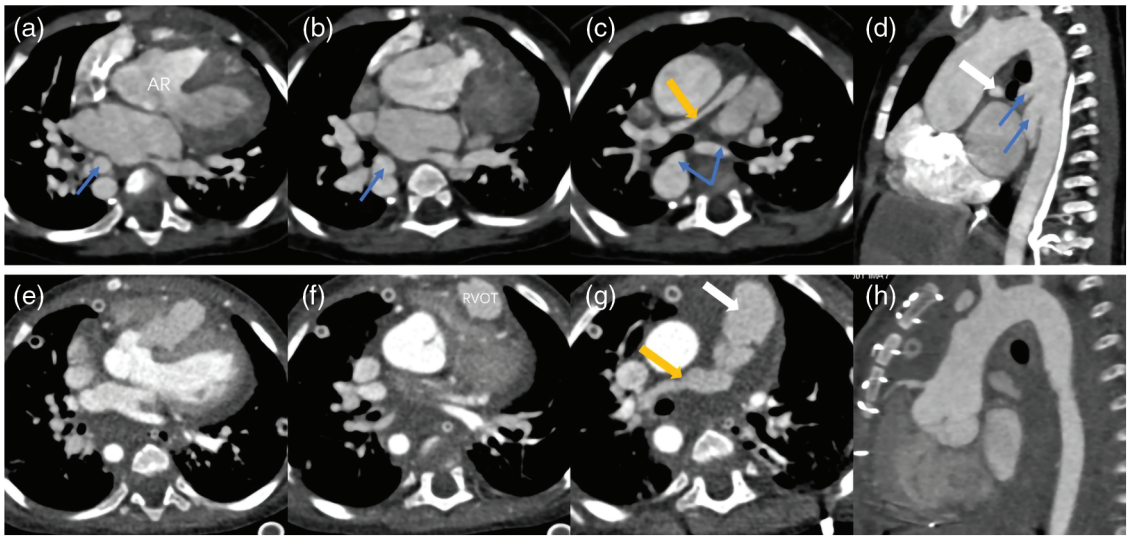

Figure 5: Two sets images of a PA patient who underwent surgery. The images of (a–d) were pre-operation and (e–h) were post-operation. The surgery reconstructed the right ventricular outflow tract (RVOT) and pulmonary trunk (white arrow), repaired the aortic riding (AR), disconnected the MAPCAs (blue arrows) and expanded the right pulmonary artery (yellow arrow) and left pulmonary artery (not shown) by using the disconnected MAPCAs. This patient was accompanied with right aortic arch

Table 2: The ICC scores of two radiologists

Index	Radiologist 1	Radiologist 2	ICC	95% CI
McGoon	1.53 ± 0.53	1.51 ± 0.60	0.943	0.885–0.972
PAI	171.90 ± 105.60	167.56 ± 114.50	0.969	0.938–0.985
TNPAI	174.87 ± 69.18	168.31 ± 78.20	0.947	0.825–0.985

Abbreviations: PAI, pulmonary arterials index; TNPAI, total neopulmonary arterial index.

3.4 Comparison between TTE and DSCT for Diagnosing Intracardiac or Extracardiac Deformities

Of the deformities, 182, 162, and 13 intracardiac, extracardiac, and other major malformations were diagnosed (Table 3). DSCT showed a better diagnostic performance in extracardiac deformities (154 *vs.* 117, $p < 0.001$), whereas TTE could diagnose intracardiac deformities better (159 *vs.* 139, $p = 0.005$). For other major malformations, TTE and DSCT did not show a significant difference ($p = 0.336$). Moreover, DSCT could demonstrate cardiac vessels better than TTE, especially PDA and MAPCAs. The sensitivities for PDA and MAPCAs were 91.5% (DSCT) *vs.* 93.2% (TTE) and 94.7% (DSCT) *vs.* 78.9% (TTE), respectively. While the specificities were 100% (DSCT) *vs.* 26.7% (TTE) and 100% *vs.* 82.9%, respectively. TTE could diagnose valve deformities better, including valve malformation and valvular inadequacy. The sensitivities and specificities were 100% (TTE) *vs.* 31.3% (DSCT) and 84.1% (TTE) *vs.* 100% (DSCT), respectively (Table 4).

Table 3: All malformation diagnosed by TTE, DSCT and final diagnoses (n = 79)

Type of malformation	Final diagnoses	DSCT diagnoses				TTE diagnoses			
		TP	TN	FP	FN	TP	TN	FP	FN
Intra-cardiac deformities									
VSD	75	71	4	0	4	73	3	1	2
ASD/PFO	47	27	31	1	20	35	19	13	12
Aorta overriding	44	36	22	13	8	35	28	7	9
Valve abnormities	16	5	63	0	11	16	53	10	0
Extra-cardiac deformities									
PDA	59	54	20	0	5	55	4	11	9
MAPCAs	38	36	41	0	2	30	34	7	8
RAA	26	26	53	0	0	17	51	2	9
DAA	2	2	77	0	0	0	77	0	2
PSVC	14	14	64	1	0	8	63	2	6
ASA	13	13	65	1	0	1	65	1	12
CAD	10	9	68	1	1	6	65	4	4
Other major malformations									
DORV	7	3	70	2	4	5	70	2	2
SV	4	4	73	2	0	4	75	0	0
SV + SA	2	1	77	0	1	1	77	0	1

Abbreviations: TP, true positive finding; FN, false negative finding; TN, true negative finding; FP, false positive finding; VSD, ventricular septal defect; ASD, atrial septal defect; PFO, patent foramen ovale; DORV, double outlet right ventricle; SV, single ventricle; SA, single atrium; PDA, patent ductus arteriosus; MAPCAs, major aortopulmonary collateral arterials; RAA, right aortic arch; DAA, double aortic arch; PSVC, persistent superior vena cava; ASA, aberrant subclavian artery; CAD, coronary artery deformities; PAPVC, partial anomalous pulmonary venous connection.

3.5 Radiation Dose Estimation

The dose length product and volume CT dose index of the different groups are classified by age (Table 5). The effective doses were 0.85 ± 0.39, 0.75 ± 0.58, 0.66 ± 0.45 and 0.58 ± 0.32 mSv in patients <4 months, 4–12 months, 1–5 years and 5–10 years, respectively.

Table 4: The diagnostic accuracy of DSCT and TTE (n = 79)

Type of malformation	DSCT diagnoses				TTE diagnoses			
	Sen (%)	Spe (%)	PPV (%)	NPV (%)	Sen (%)	Spe (%)	PPV (%)	NPV (%)
Intra-cardiac deformities								
VSD	94.7	100	100	50.0	97.3	75.0	98.6	60.0
ASD/PFO	57.4	96.9	96.4	60.8	74.5	59.4	72.9	61.3
Aorta overriding	81.8	62.9	73.3	79.5	79.5	80.0	83.3	75.7
Valve abnormities	31.3	100	73.5	85.1	100	84.1	61.5	100
Extra-cardiac deformities								
PDA	91.5	100	100	80.0	93.2	26.7	83.3	30.8
MAPCAs	94.7	100	100	95.3	78.9	82.9	81.1	81.0
RAA	100	100	100	100	65.4	96.2	89.4	85.0
DAA	100	100	100	100	0	100	0	97.5
PSVC	100	98.5	93.3	100	57.1	96.9	80.0	91.3
ASA	100	98.5	92.9	100	7.7	98.5	50.0	84.4
CAD	90.0	98.6	90.0	98.6	66.7	94.2	60.0	94.2
PAPVC	100	100	100	100	100	98.7	50	100
Other major malformations								
DORV	42.9	97.2	60.0	94.6	71.4	97.2	71.4	97.2
SV	100	97.3	66.7	100	100	100	100	100
SV + SA	50.0	100	100	98.7	50.0	100	100	98.7

Abbreviations: Sen, sensitivity; Spec, specificity; PPV, positive predictive value; NPV, negative predictive value; VSD, ventricular septal defect; ASD, atrial septal defect; PFO, patent foramen ovale; DORV, double outlet right ventricle; PDA, patent ductus arteriosus; MAPCAs, major aortopulmonary collateral arterials; RAA, right aortic arch; DAA, double aortic arch; PSVC, persistent superior vena cava; ASA, aberrant subclavian artery; CAD, coronary artery deformities; SV, single ventricle; SA, single atrium; PAPVC, partial anomalous pulmonary venous connection.

Table 5: Radiation dose estimation in different age groups

	<4 months	4 months to 1 year	1 year to 5 years	5 years to 10 years
Patients, n (%)	6 (7.6)	22 (27.8)	32 (40.5)	12 (15.2)
CTDIvol (mGy)	0.96 ± 0.52	1.89 ± 2.69	1.59 ± 1.86	1.23 ± 1.08
DLP (mGy.cm)	22.03 ± 9.89	28.94 ± 22.48	36.96 ± 25.01	44.98 ± 24.45
ED (mSv)	0.85 ± 0.39	0.75 ± 0.58	0.66 ± 0.45	0.58 ± 0.32

Abbreviations: CTDIvol, volume CT dose index; DLP, dose-length product; ED, effective dose.

4 Discussion

Pulmonary atresia patients are often associated with a variety of intracardiac and extracardiac malformations. Different PA patients need different care and treatments. This study has major discoveries as follows: (1) Different groups of PA patients have different surgical indices (McGoon ratio and PAI) and DSCT can demonstrate NPA and MAPCAs well. Therefore, the surgical indices could be roughly

calculated to design treatments. (2) DSCT has a better diagnostic performance for extracardiac deformities than that of TTE.

PA is a complex CHD that is not just one type. However, up to now, most studies only focused on one type of PA, that is, PA/VSD, PA/VSD/MAPCAs, or PA with intact ventricular septum [20]. And it is believed that no study comparing different types of PA currently exists. Additionally, only a few studies showed the values of DSCT in patients with PA. The results of this study showed that the common clinical data were not significantly different except for age and respiratory rate. However, all these data indicated that patients were in a poor situation and indicated that they needed timely treatment. For example, preoperative SpO_2 was low and symptoms were obvious and critical. This may be explained by the fact that PA is a complex and severe CHD which makes them in such a poor situation. Meanwhile, the mean McGoon, PAI and TNPAI of all patients were in a level that could enable patients to undergo surgery. This is consistent with the fact that most patients in the three groups underwent surgical treatments. However, the surgical indices (McGoon ratio and PAI), as well as various treatments among the three groups, were significantly different.

PA/VSD had a higher McGoon ratio and PAI and all patients underwent surgical treatments. The other two groups had a lower McGoon ratio and PAI. Consequently, more patients only underwent CCA examinations or palliative surgery. Different McGoon ratios and PAI indicate the development of the NPA situation. A higher ratio means a lower risk of surgery and a better outcome [21,22]. Thus, patients with low surgical indices could not undergo the one-stage surgery, which helps to explain the fact that more patients in the two latter groups did not undergo one-stage surgery in this study. However, TNPAI was not significantly different in the latter two groups, which may be because of the small sample size (only eight patients had MAPCAs in the group of PA with other major malformations). DSCT could depict NPA and MAPCAs well and display them in three dimensions with the help of postprocessing techniques. Thus, their diameter could be roughly measured. On the basis of this fact, surgical plan could be roughly designed. Moreover, DSCT could show the stenosis places and the concrete origin locations of MAPCAs which are important for the surgical plan of patients with PA/VSD/MAPCAs. This study demonstrates the value of DSCT used to design the treatment plans without undergoing CCA. CCA can be used to assess the situation of NPA, MAPCAs and the distribution of pulmonary artery branches [23]. But it is invasive and expensive. What's more, CCA with the highest patient radiation dose has an insurmountable defect for infants and children because they are more vulnerable to radiation [24].

Compared with echocardiography, DSCT demonstrates extracardiac deformities better, while TTE diagnoses intracardiac deformities (especially valve deformities) better in this study, which is consistent with the previous studies [25,26]. Complex congenital heart diseases are often accompanied by not only intracardiac malformation but also extracardiac malformation which needs more than one imaging modalities to get a correct diagnosis. TTE is the routine examination for heart diseases, especially for CHD, which could investigate the intracardiac deformities and hemodynamics well. Nonetheless, TTE is not very useful for extracardiac deformities for its limited acoustic window and is dependent on the operators heavily [27]. When patients have simple CHD involving no complex extracardiac malformations and having definite diagnosis (such as atrial/ventricular septal defects, patent ductus arteriosus, Ebstein's anomaly and so on), echocardiography diagnoses could be decisive. However, when incorporated with complex extracardiac malformations, TTE is not sufficient enough. Other examination modalities should be used to cover the shortage of TTE [28,29]. CCA is identified as "*gold standard*" for the blood supply of the lungs. But it also has some shortcomings as illustrated above. Cardiac MRI can measure hemodynamics, either. But it is demanding for motionlessness and time which is difficult for young patients and patients with CHD. Besides, the spatial resolution is poorer and it has less contribution to submillimeter vessels and coronary vessels compared with CT [30,31].

All of these insufficiencies can be complemental by DSCT. With the development of DSCT, it has increasingly been applied to CHD. It can portray the extra-cardiac deformities well and provide more mediastinal anatomy information for surgeon to design surgical plans before the operation owing to its high-density resolution and powerful postprocessing techniques. Moreover, its high temporal resolution enables its use in patients with high heart rate [32] by using two independent X-ray tubes and corresponding detectors. Additionally, as our results show, its radiation dose has been reduced to *as low as reasonably achievable* [14], which makes it suitable for young patients. Thus, DSCT plays an irreplaceable role in the diagnosis of PA and treatment and management design.

Several limitations exist in this study. First, all patients came from a single center, which leads to selection bias and a relatively small sample size, especially for the group of PA with other major malformation, which influenced the data collection and analysis of this study. Hence, further studies with larger samples coming from multicenter should be conducted. Second, the radiation dose has reduced greatly, although still exists, which helps reduce the injury for young patients, with the help of technique development. Third, the outcomes of the different groups with long-term follow-up, which may aid in further management of this disease, were not tracked.

5 Conclusion

Different PA groups have different McGoon and PAI. TTE can diagnose intracardiac deformities well, whereas DSCT can demonstrate extracardiac malformation better and give more information to optimize the surgical design. More than one imaging modality should be used to make a correct diagnosis when clinically suspecting PA.

Authorship: The authors confirm their contribution to the paper as follows: QWL participated in the study design, data collection, performed the statistical analysis, and drafted the manuscript. YZG contributed to study design, and contributed to preparation, editing and review of the manuscript. XZZ participated in data collection, and contributed to quality control of data and analysis. SK and JL contributed to preparation, editing and review of the manuscript. LX and SMT participated in data acquisition and analysis. All authors read and approved the final manuscript.

Ethics Approval: This study was approved by the Institutional Ethics Committee of West China Hospital, Sichuan University (Chengdu, Sichuan, China; No. 14-163), with a waiver of informed consent due to the retrospective nature.

Funding Statement: This study has received funding by Sichuan Science and Technology Program (2020YJ0229) and 1·3·5 Project for Disciplines of Excellence, West China Hospital, Sichuan University (ZYGD18013). The funding sources had no role of the study design; collection; analysis and interpretation of data; in the writing of the report; and in the decision to submit the article for publication.

Conflicts of Interest: The authors declare that they have no conflicts of interest to report regarding the present study.

References

1. Kawel, N., Valsangiacomo-Buechel, E., Hoop, R., Kellenberger, C. J. (2010). Preoperative evaluation of pulmonary artery morphology and pulmonary circulation in neonates with pulmonary atresia–usefulness of MR angiography in clinical routine. *Journal of Cardiovascular Magnetic Resonance, 12(1),* 52. DOI 10.1186/1532-429x-12-52.
2. Tchervenkov, C. I., Roy, N. (2000). Congenital heart surgery nomenclature and database project: Pulmonary atresia–ventricular septal defect. *The Annals of Thoracic Surgery, 69(3),* S97–S105. DOI 10.1016/s0003-4975(99)01285-0.

3. Hu, B. Y., Shi, K., Deng, Y. P., Diao, K. Y., Xu, H. Y. et al. (2017). Assessment of tetralogy of fallot-associated congenital extracardiac vascular anomalies in pediatric patients using low-dose dual-source computed tomography. *BMC Cardiovascular Disorders, 17(1),* 285. DOI 10.1186/s12872-017-0718-8.
4. Zhao, Q. M., Liu, F., Wu, L., Ma, X. J., Niu, C. et al. (2019). Prevalence of congenital heart disease at live birth in China. *The Journal of Pediatrics, 204,* 53–58. DOI 10.1016/j.jpeds.2018.08.040.
5. Leonard, H., Derrick, G., O'Sullivan, J., Wren, C. (2000). Natural and unnatural history of pulmonary atresia. *Heart, 84(5),* 499–503. DOI 10.1136/heart.84.5.499.
6. Soquet, J., Barron, D. J., d'Udekem, Y. (2019). A review of the management of pulmonary atresia, ventricular septal defect, and major aortopulmonary collateral arteries. *The Annals of Thoracic Surgery, 108(2),* 601–612. DOI 10.1016/j.athoracsur.2019.01.046.
7. Bull, K., Somerville, J., Ty, E., Spiegelhalter, D. (1995). Presentation and attrition in complex pulmonary atresia. *Journal of the American College of Cardiology, 25(2),* 491–499. DOI 10.1016/0735-1097(94)00364-v.
8. Thiene, G., Frescura, C., Bini, R. M., Valente, M., Gallucci, V. (1979). Histology of pulmonary arterial supply in pulmonary atresia with ventricular septal defect. *Circulation, 60(5),* 1066–1074. DOI 10.1161/01.cir.60.5.1066.
9. Liao, P. K., Edwards, W. D., Julsrud, P. R., Puga, F. J., Danielson, G. K. et al. (1985). Pulmonary blood supply in patients with pulmonary atresia and ventricular septal defect. *Journal of the American College of Cardiology, 6(6),* 1343–1350. DOI 10.1016/s0735-1097(85)80223-0.
10. Reddy, V. M., McElhinney, D. B., Amin, Z., Moore, P., Parry, A. J. et al. (2000). Early and intermediate outcomes after repair of pulmonary atresia with ventricular septal defect and major aortopulmonary collateral arteries: Experience with 85 patients. *Circulation, 101(15),* 1826–1832. DOI 10.1161/01.cir.101.15.1826.
11. Mi, Y. P., Chau, A. K., Chiu, C. S., Yung, T. C., Lun, K. S. et al. (2005). Evolution of the management approach for pulmonary atresia with intact ventricular septum. *Heart, 91(5),* 657–663. DOI 10.1136/hrt.2004.033720.
12. Mainwaring, R. D., Patrick, W. L., Roth, S. J., Kamra, K., Wise-Faberowski, L. et al. (2018). Surgical algorithm and results for repair of pulmonary atresia with ventricular septal defect and major aortopulmonary collaterals. *The Journal of Thoracic and Cardiovascular Surgery, 156(3),* 1194–1204. DOI 10.1016/j.jtcvs.2018.03.153.
13. Han, B. K., Rigsby, C. K., Hlavacek, A., Leipsic, J., Nicol, E. D. et al. (2015). Computed tomography imaging in patients with congenital heart disease part I: Rationale and utility. an expert consensus document of the society of cardiovascular computed tomography (SCCT): Endorsed by the society of pediatric radiology (SPR) and the north American society of cardiac imaging (NASCI). *Journal of Cardiovascular Computed Tomography, 9(6),* 475–492. DOI 10.1016/j.jcct.2015.07.004.
14. Shi, K., Yang, Z. G., Xu, H. Y., Zhao, S. X., Liu, X. et al. (2016). Dual-source computed tomography for evaluating pulmonary artery in pediatric patients with cyanotic congenital heart disease: Comparison with transthoracic echocardiography. *European Journal of Radiology, 85(1),* 187–192. DOI 10.1016/j.ejrad.2015.11.002.
15. Koplay, M., Kizilca, O., Cimen, D., Sivri, M., Erdogan, H. et al. (2016). Prospective ECG-gated high-pitch dual-source cardiac CT angiography in the diagnosis of congenital cardiovascular abnormalities: Radiation dose and diagnostic efficacy in a pediatric population. *Diagnostic and Interventional Imaging, 97(11),* 1141–1150. DOI 10.1016/j.diii.2016.03.014.
16. Yin, L., Lu, B., Han, L., Wu, R. Z., Johnson, L. et al. (2011). Quantitative analysis of pulmonary artery and pulmonary collaterals in preoperative patients with pulmonary artery atresia using dual-source computed tomography. *European Journal of Radiology, 79(3),* 480–485. DOI 10.1016/j.ejrad.2010.04.032.
17. Chaosuwannakit, N., Makarawate, P. (2018). The value of dual-source multidetector-row computed tomography in determining pulmonary blood supply in patients with pulmonary atresia with ventricular septal defect. *Folia Morphologica, 77(1),* 116–122. DOI 10.5603/FM.a2017.0062.
18. Deak, P. D., Smal, Y., Kalender, W. A. (2010). Multisection CT protocols: Sex- and age-specific conversion factors used to determine effective dose from dose-length product. *Radiology, 257(1),* 158–166. DOI 10.1148/radiol.10100047.
19. Preface, Executive Summary and Glossary (2007). *Annals of the ICRP, 37(2–4),* 331–332. DOI 10.1016/j.icrp.2007.10.003.

20. Cohen, J., Binka, E., Woldu, K., Levasseur, S., Glickstein, J. et al. (2019). Myocardial strain abnormalities in fetuses with pulmonary atresia and intact ventricular septum. *Ultrasound in Obstetrics & Gynecology, 53(4),* 512–519. DOI 10.1002/uog.19183.
21. Nakata, S., Imai, Y., Takanashi, Y., Kurosawa, H., Tezuka, K. et al. (1984). A new method for the quantitative standardization of cross-sectional areas of the pulmonary arteries in congenital heart diseases with decreased pulmonary blood flow. *The Journal of Thoracic and Cardiovascular Surgery, 88(4),* 610–619. DOI 10.1016/S0022-5223(19)38300-X.
22. Karaca-Altintas, Y., Laux, D., Gouton, M., Bensemlali, M., Roussin, R. et al. (2020). Nakata index above 1500 mm^2/m^2 predicts death in absent pulmonary valve syndrome. *European Journal of Cardio-Thoracic Surgery, 57(1),* 46–53. DOI 10.1093/ejcts/ezz167.
23. Reddy, V. M., Petrossian, E., McElhinney, D. B., Moore, P., Teitel, D. F. et al. (1997). One-stage complete unifocalization in infants: When should the ventricular septal defect be closed? *The Journal of Thoracic and Cardiovascular Surgery, 113(5),* 858–866. DOI 10.1016/s0022-5223(97)70258-7.
24. Bacher, K., Bogaert, E., Lapere, R., de Wolf, D., Thierens, H. (2005). Patient-specific dose and radiation risk estimation in pediatric cardiac catheterization. *Circulation, 111(1),* 83–89. DOI 10.1161/01.Cir.0000151098.52656.3a.
25. Mei, M., Nie, J., Yang, Z. S., Sun, H. W., Wang, H. et al. (2019). Comparison of echocardiography and 64-slice spiral computed tomography in the diagnosis of congenital heart disease in children. *Journal of Cellular Biochemistry, 120(3),* 3969–3977. DOI 10.1002/jcb.27682.
26. Zhao, Q., Wang, J., Yang, Z. G., Shi, K., Diao, K. Y. et al. (2019). Assessment of intracardiac and extracardiac anomalies associated with coarctation of aorta and interrupted aortic arch using dual-source computed tomography. *Scientific Reports, 9(1),* 11656. DOI 10.1038/s41598-019-47136-1.
27. Novaes, J. Y., Zamith, M. M., Araujo Júnior, E., Barreto, E. Q., Barros, F. S. et al. (2016). Screening of congenital heart diseases by three-dimensional ultrasound using spatiotemporal image correlation: Influence of professional experience. *Echocardiography, 33(1),* 99–104. DOI 10.1111/echo.13002.
28. Guidelines for the Management of Congenital Heart Diseases in Childhood and Adolescence (2017). *Cardiology in the Young, 27(S3),* S1–S105. DOI 10.1017/s1047951116001955.
29. Stout, K. K., Daniels, C. J., Aboulhosn, J. A., Bozkurt, B., Broberg, C. S. et al. (2019). 2018 AHA/ACC guideline for the management of adults with congenital heart disease: A report of the American college of cardiology/American heart association task force on clinical practice guidelines. *Circulation, 139(14),* e698–e800. DOI 10.1161/cir.0000000000000603.
30. Dacher, J. N., Barre, E., Durand, I., Hazelzet, T., Brasseur-Daudruy, M. et al. (2016). CT and MR imaging in congenital cardiac malformations: Where do we come from and where are we going? *Diagnostic and Interventional Imaging, 97(5),* 505–512. DOI 10.1016/j.diii.2016.02.009.
31. Lloyd, D. F. A., Goreczny, S., Austin, C., Hussain, T., Qureshi, S. A. et al. (2018). Catheter, MRI and CT imaging in newborns with pulmonary atresia with ventricular septal defect and aortopulmonary collaterals: Quantifying the risks of radiation dose and anaesthetic time. *Pediatric Cardiology, 39(7),* 1308–1314. DOI 10.1007/s00246-018-1895-7.
32. Flohr, T. G., McCollough, C. H., Bruder, H., Petersilka, M., Gruber, K. et al. (2006). First performance evaluation of a dual-source CT (DSCT) system. *European Radiology, 16(2),* 256–268. DOI 10.1007/s00330-005-2919-2.